

Mesoscopic spin polarization and nuclear electronic resonance

A. G. Aronov and Yu. B. Lyanda-Geller

A. F. Ioffe Physicotechnical Institute, Academy of Sciences of the USSR

(Submitted 7 June 1990)

Pis'ma Zh. Eksp. Teor. Fiz. **52**, No. 1, 663–666 (10 July 1990)

The local spin polarization of electrons in an electric field leads to the appearance of a nuclear electric resonance and localized electron spin resonance in a bulk sample.

In media with a lowered symmetry a spin-orbit interaction causes a spin polarization of electrons as a result of the flow of current.¹

A random distribution of impurities and defects in conductors leads to a local distribution of the spatial symmetry (the local mesoscopic effect) and to a spin polarization in an electric field in regions where the electron is scattered coherently by a random potential. The physical reason for such a local spin polarization is the spin relaxation of the current carriers. The average polarization of a macroscopic sample in this case is zero since the spins of the individual parts of the sample cancel each other.

The principal result on which we wish to focus attention in this letter¹⁾ is the fact that the mesoscopic spin polarization can be observed in a massive sample, despite the fact that its macroscopic polarization is absent under conditions when the square of the local spin density can be observed directly in an experiment. This can be done, for example, in a nuclear electric resonance predicted by us¹ or a localized-spin resonance excited by an electric field.

The local electron spin at a given point in the sample, which arises as a result of the action of an rf electric field E_ω , varies with time at a frequency ω . A hyperfine interaction of electron and nuclear spins or an exchange interaction with a localized spin causes transitions between the nuclear (electron) magnetic sublevels in a static magnetic field \mathbf{H} , which are excited by an electric field. The intensity maximum of these transitions occurs at a frequency of the nuclear magnetic (or electron spin) resonance.

The intensity of the resonance in a bulk sample is proportional to the spatial fluctuations of the spin density at a given point $\int \langle S_\perp^2(\mathbf{r}) \rangle d\mathbf{r}$ (S_\perp is the spin component at right angles to the external magnetic field). The quantity $\langle S_\perp^2(\mathbf{r}) \rangle$, in contrast with the average spin, has the same sign for all local regions, and therefore the resonance intensity is proportional to the volume of the sample.

To calculate the spin density fluctuations, we can use the graphic impurity technique. Examples of the important diagrams which give $\int \langle S_\perp^2(\mathbf{r}) \rangle d\mathbf{r}$ with a large momentum transfer at the vertices and which correspond to the local spin operator are shown in Fig. 1. The diagrams such as those in Fig. 1a, which contain two diffusons and vertices, in which the sign of the imaginary part of the Green's function changes,

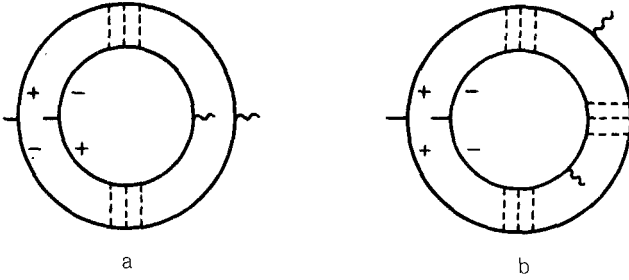


FIG. 1. Diagrams showing the spin density fluctuations. (a) Two-diffuson diagrams in which the imaginary part of the Green's function reverses sign at the vertices; (b) three-diffuson (three-cooperon) diagrams. The vertices on the left side correspond to the spin operators and those on the right (the wavy line) correspond to the operators which interact with the electric field.

describe the onset of polarization as a result of spin-orbit coupling due to the real absorption of the electric component of the microwave field. Similar diagrams which contain two cooperons are small in the parameter $1/p_F l$, where p_F is the Fermi momentum, and l is the mean free path. Diagrams in which the sign at the vertices does not change,²⁾ including the diagram in Fig. 1b, describe the electron polarization by the electric field without absorption. These diagrams are physically similar to the diagrams for the correlation function of the real parts of the magnetic susceptibility. The diagrams with diffusons and those with cooperons in this case should be taken into account in these three-ladder diagrams. These components differ in a static magnetic field.

Below we present the results of calculations of $\langle S_{\perp}^2(\mathbf{r}) \rangle$ for a uniform electric field. After analytic continuation in the temperature diagram technique we can write the contribution from the diagrams with two diffusons in the form

$$\langle S_{\perp}^2(\mathbf{r}) \rangle = A \int_{-\infty}^{+\infty} \frac{dx}{2\pi} \int_{-\infty}^{+\infty} \frac{dx'}{2\pi} f'(x) \cdot f'(x') \sum_{\mathbf{q}} [D_{00}^2(x+x') - D_{10}^2(x+x') + D_{00}(x+x')D_{00}(0) - D_{10}(x+x')D_{10}(0)], \quad (1)$$

where $A = 2\pi v \tau (eE_{\alpha} V_F)^2 / T^2 d$, v is the density of states, τ is the momentum relaxation time, d is the dimension of space $f'(x) = \frac{1}{4} \cosh^{-2}(x/2)$, and the values of D_{jm} , which determine the spin structure of the diffuson (cooperon) in the presence of Larmor precession and the spin-orbit mechanism of the spin relaxation, are given by

$$D_{jm}(x) = (Dq^2/T + ix + im\alpha_H + \frac{4}{3}j\alpha_{s0} + \alpha_0)^{-1}. \quad (2)$$

Here $\alpha_H = \omega_H/T$, ω_H is the Larmor frequency, T is the temperature, $\alpha_{s0} = (L_T/L_{s0})^2 L_T = (D/T)^{1/2}$, D is the diffusion coefficient, $L_{s0} = (D\tau_{s0})^{1/2}$, τ_{s0} is the spin relaxation time, $\alpha_0 = 1/T\tau_0 \ll 1$, and τ_0 is the inelastic scattering time. The result of calculation of the diagrams with three diffusons is

$$\begin{aligned}
\langle \mathbf{S}_{\perp}^2(\mathbf{r}) \rangle &= 4A \int_{-\infty}^{+\infty} \frac{dx}{2\pi} \int_{-\infty}^{+\infty} \frac{dx'}{2\pi} f'(x) f'(x') \sum_{\mathbf{q}} Dq^2 / T \\
&\times [D_{00}^3(x+x') \\
&- D_{10}^3(x+x') + \frac{3}{4} (D_{00}(x+x') - D_{10}(x+x')) (D_{11}(x+x') - D_{1-1}(x+x'))^2],
\end{aligned} \tag{3}$$

When $\alpha_{s_0} \ll 1$, the principal contribution to $\langle \mathbf{S}_{\perp}^2(\mathbf{r}) \rangle$ comes from the two-diffuson diagrams which contain only D_{j_0} and which do not depend on the magnetic field. As a result, the Larmor precession is inconsequential and

$$\langle \mathbf{S}_{\perp}^2(\mathbf{r}) \rangle = \frac{E^2 L_T}{48\pi} \begin{cases} \frac{\sigma L_T}{D^2 L_0} (\sqrt{1 + \frac{4}{3} \frac{\tau_0}{\tau_{s_0}}} - 1) & (d=3) \\ \frac{gL_T}{D^2} \ln(1 + \frac{4\tau_0}{3\tau_{s_0}}) & (d=2), \end{cases} \tag{4}$$

where $\mathbf{S}_{\perp}(\mathbf{r})$ for $d=2$ is the two-dimensional spin density, σ and g are respectively the conductivity and the conductance of the film, and $L_0 = (D\tau_0)^{1/2}$.

In the case of strong spin-orbit coupling $\alpha_{s_0} \gg 1$ $\langle \mathbf{S}_{\perp}^2(\mathbf{r}) \rangle$ can be determined from the diagram in Fig. 1a and in Fig. 1b. In the two-dimensional case we have

$$\langle \mathbf{S}_{\perp}^2(\mathbf{r}) \rangle = \frac{1}{48\pi} \frac{gE^2}{D^2} L_T^2 [\ln(T\tau_{\varphi}) + 6 + f_2(\alpha_{s_0}, \beta)], \tag{5}$$

where the logarithmic term is related only to the two-diffuson diagrams, $\beta = L_T/L_H$, $L_H = (\hbar c/eH)^{1/2}$ is the magnetic length, and the function $f_2(\alpha_{s_0}, \beta)$, which is associated with the three-cooperon components, is given by

$$f_2(\alpha_{s_0}, \beta) = \begin{cases} 4 - 8L_T^4/5L_H^4 & (L_H \gg L_T, L_{s_0}) \\ 6\pi L_H^2/L_T^2 & (L_{s_0} \ll L_H \ll L_T) \\ \frac{63\zeta(3)}{\pi} L_H^4/L_{s_0}^2 L_T^2 & (L_T \gg L_{s_0} \gg L_H). \end{cases} \tag{6}$$

In the three-dimensional case, the diagrams in Figs. 1a and 1b give the same in order of magnitude contribution:

$$\langle \mathbf{S}_{\perp}^2(\mathbf{r}) \rangle = \frac{\sigma E^2}{16D^2} \frac{3L_T}{\sqrt{2}\pi^{5/2}} (\zeta(\frac{3}{2}) + f_3(\alpha_{s_0}, \beta)), \tag{7}$$

where

$$f_3(\alpha_{s_0}, \beta) = \begin{cases} \frac{3}{4} \zeta\left(\frac{3}{2}\right) - \frac{5}{4\pi} \zeta\left(\frac{5}{2}\right) L_T^4 / L_H^4 & (L_H \gg L_T, L_{s_0}) \\ \frac{8\sqrt{\pi}}{3} (2\sqrt{2} - 1) \zeta\left(\frac{3}{2}\right) L_H / L_T & (L_{s_0} \ll L_H < L_T) \\ \frac{3\sqrt{\pi}}{2} (4\sqrt{2} - 1) \zeta\left(\frac{5}{2}\right) L_H^3 / L_{s_0}^2 L_T & (L_T \gg L_{s_0} \gg L_H). \end{cases} \quad (8)$$

It can be seen from expressions (5)–(8), therefore, that at $H = 0$ the three-cooperon components are of the same order of magnitude as the diffuson components, and that the dependence on the magnetic field stems from their suppression. The characteristic magnetic fields are determined by the relation $L_H \sim L_T$.

The mesoscopic fluctuations of the local spin polarization $\langle S_z^2(\mathbf{r}) \rangle$ in the electric field account for the dependence of the nonuniform spin resonance line width on the electric field, as noted in Ref. 4. Without resorting to detailed calculations, we note that the Larmor spin precession causes this nonuniform width to change, in contrast with the intensity.

We wish to thank A. Yu. Zyuzin, D. E. Khmel'nitskiĭ, and V. I. Fal'ko for useful discussions.

¹This topic was also discussed in part in an article published in the Proceedings of the XX International Conference on Semiconductor Physics.²

²These diagrams were not included in Refs. 3 and 4, which were brought to our attention when this article was being prepared for publication.

¹A. G. Aronov and Yu. B. Lyanda-Geller, *Pis'ma Zh. Eksp. Teor. Fiz.* **50**, 398 (1989) [*JETP Lett.* **50**, 431 (1989)].

²A. G. Aronov and Yu. B. Lyanda-Geller, *Proceedings of the XX International Conference on Semiconductor Physics*, Thessaloniki (1990), in press.

³A. Yu. Zyuzin, *Europhys. Lett.* (1990), in press.

⁴Yu. V. Nazarov, *Pis'ma Zh. Eksp. Teor. Fiz.* **51**, 375 (1990) [*JETP Lett.* **51**, 426 (1990)].

Translated by S. J. Amoretty